Supplementary Information

Amorphous NiCoB-coupled $MAPbI_3$ for efficient photocatalytic hydrogen evolution

Lanxuan Jiang,[a] Yanmei Guo,[a] Shaopeng Qi,[a] Ke Zhang,[a] Jinxi Chen, [a] and Yongbing Lou[a] and Yixin Zhao[b]*

[a] School of Chemistry and Chemical Engineering, Southeast University, Nanjing, 211189, China. E-mail: lou@seu.edu.cn.

[b] School of Environmental Science and Engineering, Shanghai Jiao Tong University, Shanghai, 200240, P.R. China.

1. Experimental Section

1.1 Chemicals and Materials

Methylamine solution (MA, 30 wt% in absolute ethanol, Aladdin), PbI_2(98%, Macklin), HI (55-57 wt% in water, Aladdin), H_3PO_2 (50 wt% in water, Aladdin), H_2PtCl_6 (99%, Jiuding Chemical), tetrabutylammonium fluorophosphate ($TBAPF_6$, 98%, Shanghai Xushuo), diethyl ether ($C_4H_{10}O$, ≥ 99.7%, Sinopharm Chemical Reagent Co., Ltd, China), methylene chloride (CH_2Cl_2, ≥ 99.5%, Sinopharm Chemical Reagent Co., Ltd, China). All reagents were used without any purifications.

1.2 Synthesis of MAI

MAI was prepared by mixing MA and HI solution. Add 33 mL MA solution and 19 mL HI solution into a 100 mL flask, and keep the mixture stirring for 2 h at 0 °C. The solution was evaporated at 50 °C to obtain the MAI crude product. The obtained white powder was washed several times with diethyl ether and placed in a vacuum oven (60 °C) overnight.

1.3 Preparation of $Pt/MAPbI_3$

$Pt/MAPbI_3$ composite was achieved via a photoreduction method. Specifically, 50 mg $MAPbI_3$ and 4 mg H_2PtCl_6 were added to the prepared $MAPbI_3$-saturated solution and then exposed to visible light irradiation ($\lambda \geq 420$nm) for 2 h.

1.4 Characterization

Powder X-ray diffraction (XRD) of the samples was tested using an Ultima-IV Powder X-ray Diffraction (Rigaku, Japan) equipped with a Cu Kα incident source. The UV-vis diffuse reflectance spectra were measured using an ultraviolet−visible

(UV−vis) spectrophotometer (UV2600) (Shimadzu, Japan) and $BaSO_4$ was used as a reflectance standard. The morphology of the products was characterized by scanning electron microscopy (SEM, FEI Inspect F50). Transmission electron microscopy (TEM) images were taken by a Tecnai G2 20 transmission electron microscope (FEI, USA) at an acceleration voltage of 200 kV. X-ray photoelectron spectroscopy (XPS) measurements were performed with a Thermo Fisher Nexsa spectrometer with a Al Kα X-ray radiation. The binding energies were calibrated using C1s peak (284.8 eV). The photoluminescence (PL) spectra were obtained by a Fluoromax-4 spectrofluorometer spectrometer (Horiba, Japan) with an excitation wavelength of 500 nm. Zeta potentials were measured with a NanoBrook Omni zeta potential analyzer (Brookhaven, USA).

1.5 Electrochemical and photoelectrochemical measurements

All the electrochemical and photoelectrochemical tests were performed at the CHI-660D Electrochemical Workstation (Shanghai Chenhua). In a standard three-electrode system, a Pt sheet was used as the counter electrode and the saturated Ag/AgCl as the reference electrode. The electrolyte chosen was a dichloromethane solution of 0.1M tetrabutylammonium fluorophosphate ($TBAPF_6$). As for the fabrication of working electrode, the photocatalyst powder was ground with a drop of terpinol and smeared onto plasma-treated FTO conductive glass, then left to air dry naturally. Electrochemical impedance spectroscopy (EIS) was obtained with the test frequency range of 0.1 to 10^5 Hz. Current-voltage (I-V) curves were measured using linear sweep voltammetry (LSV) method with the scan rate of 10 mV s^{-1}. Photocurrent

response curves were obtained by irradiating the working electrode at regular intervals, using a 300 W Xe-lamp with a 420 nm cut-off filter as the light source.

1.6 The calculation of Apparent Quantum efficiency (AQE):

The light intensity of irradiation at 450 nm was measured by an optical power meter (PL-MW2000, Perfectlight, Beijing). The measured light intensity (P) was 1.86 mW cm^{-2}. The irradiation area (S) was 28.26 cm^2 and the evolution amount of H_2 (n) in 4 h was 27.8 μmol:

$$\mathrm{AQE} = \frac{2 \times \text{the number of evolved } H_2 \text{ molecules}}{\text{the number of incident photons}} \times 100\%$$

$$= \frac{2nNA}{PS\lambda/hc} \times 100\% = 1.96\ \%$$

2. Additional Data

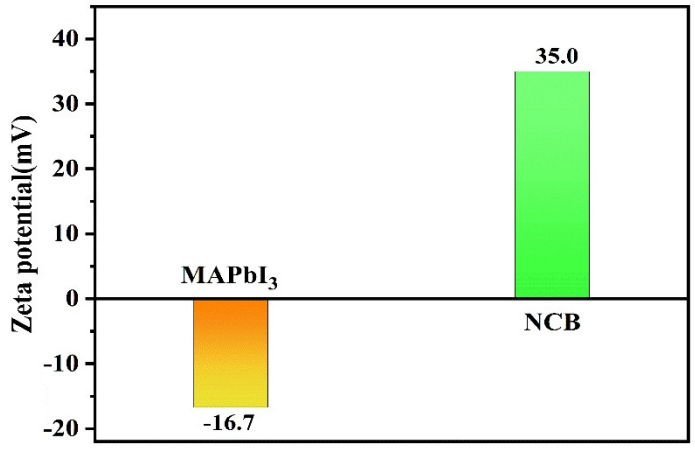

Fig. S1 Zeta potentials of $MAPbI_3$ and NiCoB

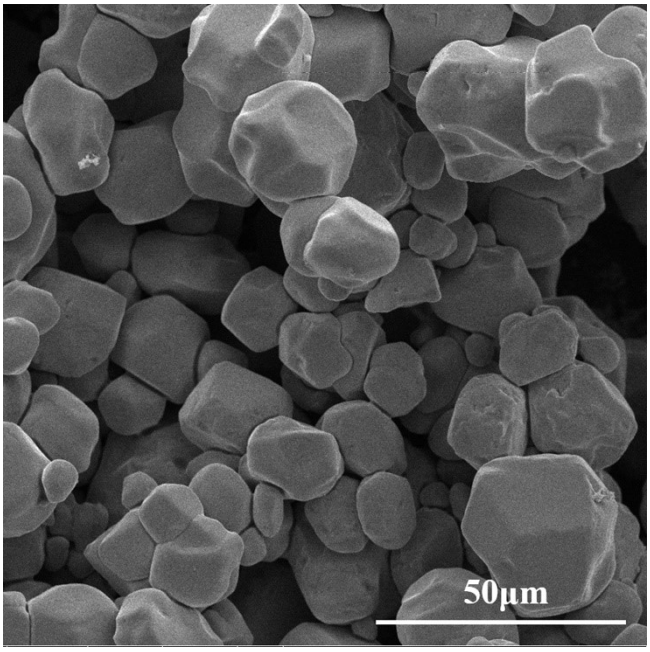

Fig. S2 SEM image of $MAPbI_3$

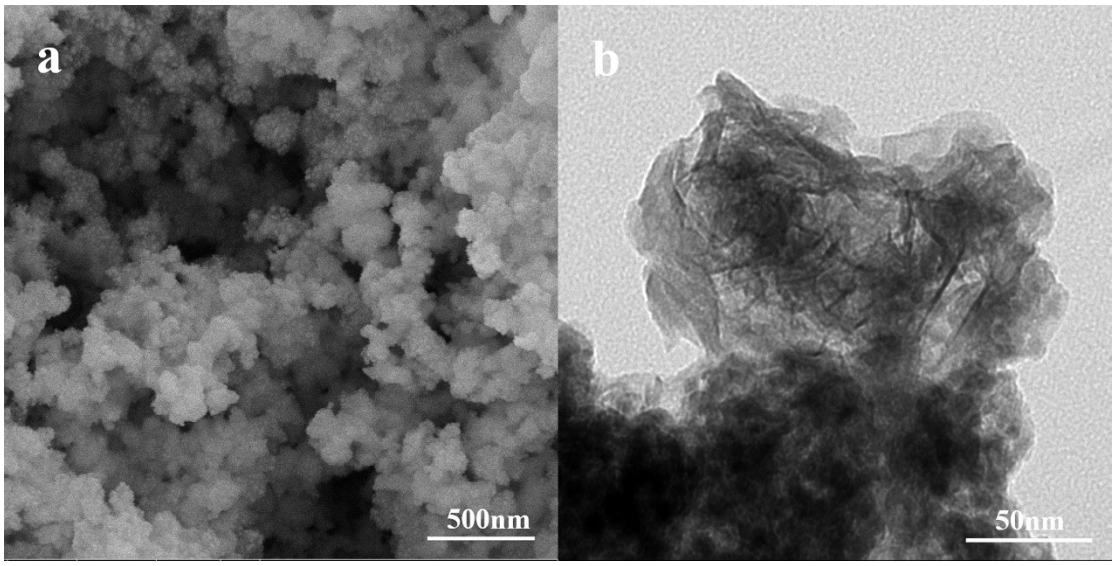

Fig. S3 (a) SEM and (b) TEM images of NiCoB

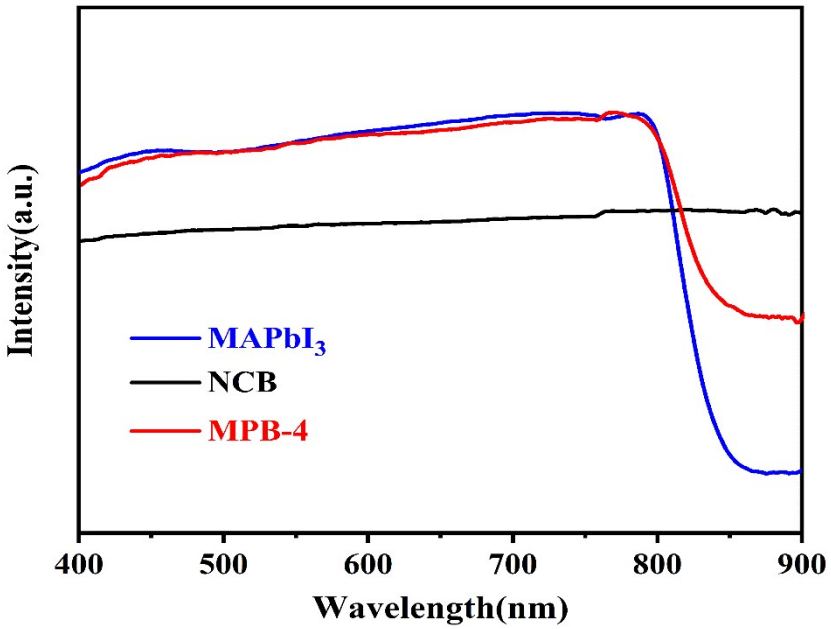

Fig. S4 UV-vis absorption spectra of NiCoB, $MAPbI_3$ and MPB-4.

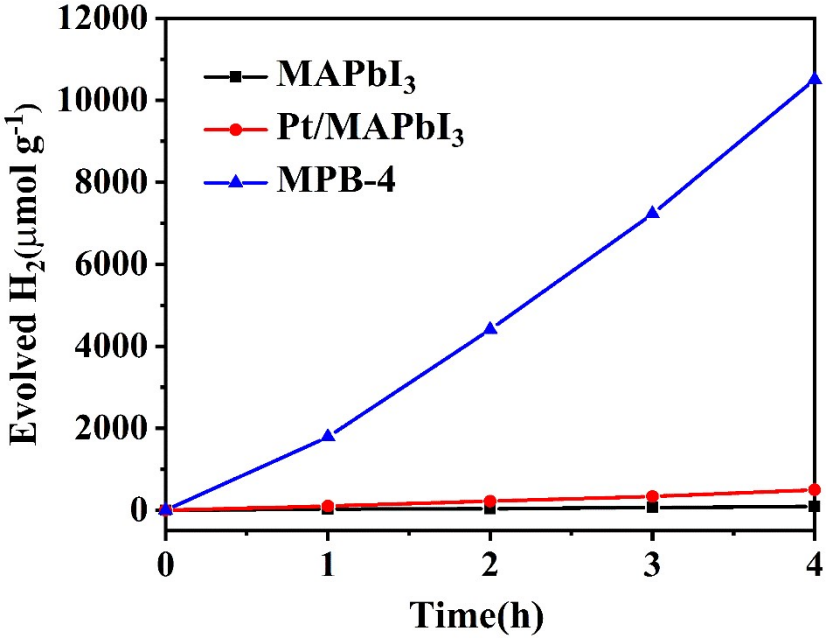

Fig. S5 Time-dependent photocatalytic H_2 production of $MAPbI_3$, $Pt/MAPbI_3$, and MPB-4.

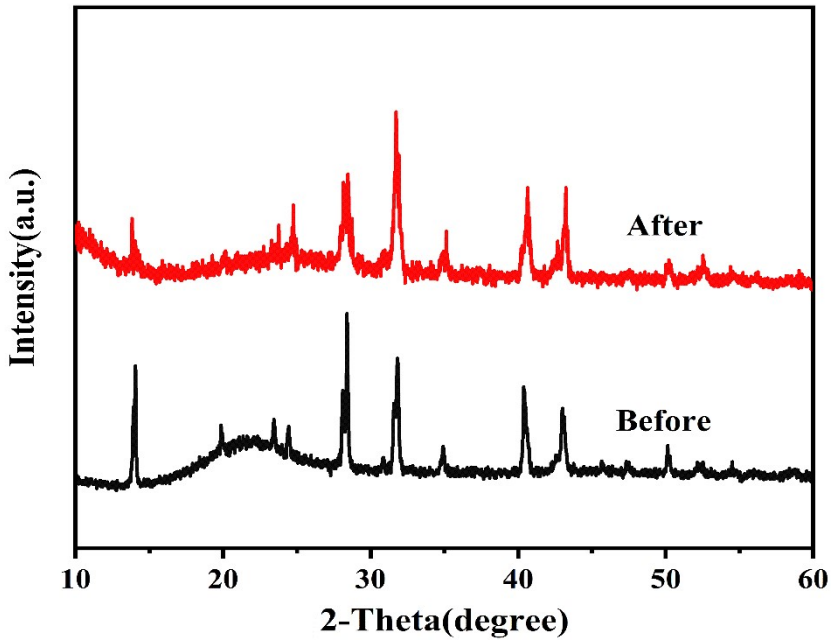

Fig. S6 XRD patterns of the MPB-4 before and after being illuminated for 24 h of photocatalytic H_2 evolution.

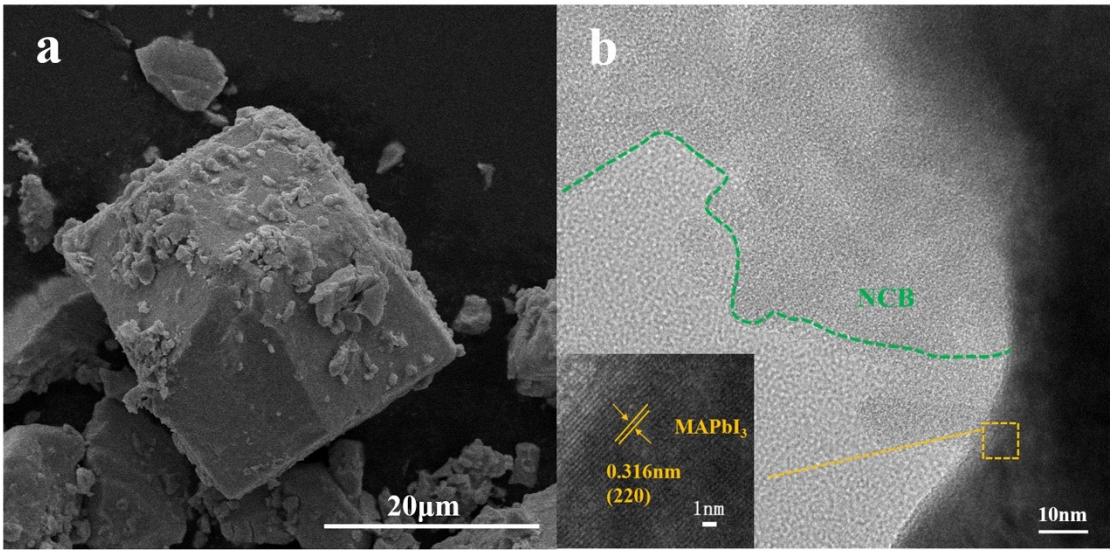

Fig. S7 SEM and HRTEM images of the MPB-4 after being illuminated for 24 h of photocatalytic H_2 evolution.

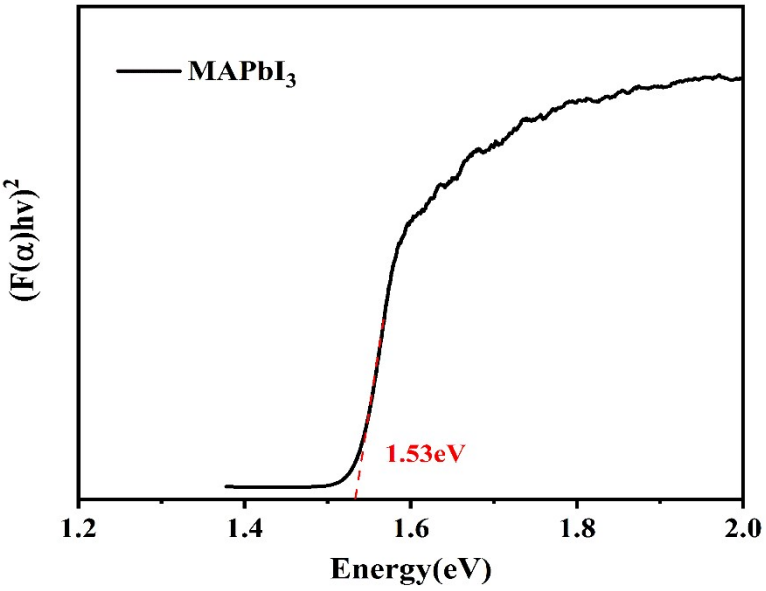

Fig. S8 The Kubelka-Munk plot of $MAPbI_3$.

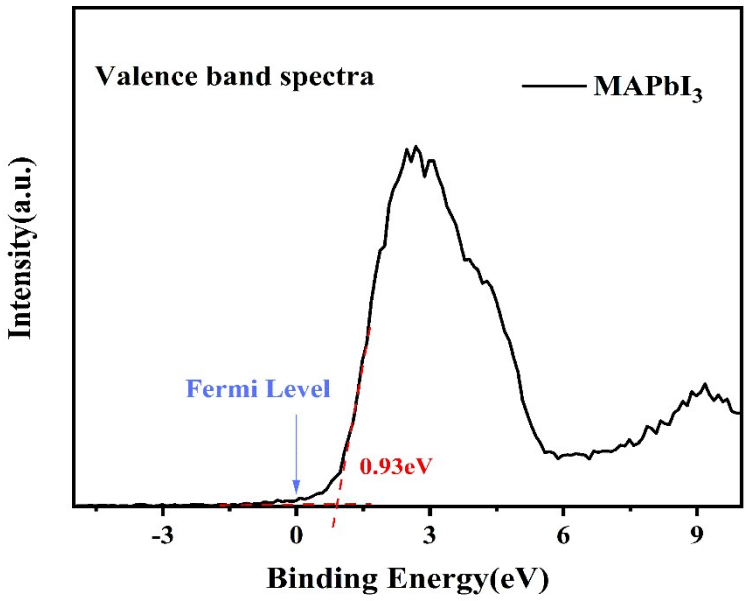

Fig. S9 Valence band XPS spectrum of $MAPbI_3$ powder.

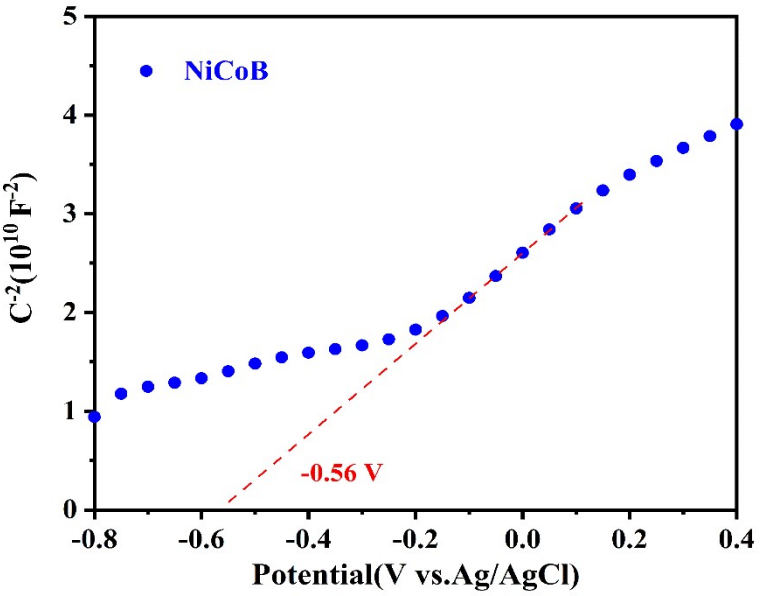

Fig. S10 Mott-Schottky curve of the NiCoB

Table S1. The comparison of photocatalytic HER performance over the NiCoB/$MAPbI_3$ and other reported $MAPbI_3$-based photocatalysts.

Catalysts	Reactant solution	Light source	H_2 evolution ($\mu mol\ g^{-1}\ h^{-1}$)	Ref.
NiCoB/$MAPbI_3$	HI/H_3PO_2 solution	300 W Xe lamp (100 mW cm^{-2}, $\lambda \geq 420$ nm)	2625.57	This work
Pt/$MAPbI_3$	HI/H_3PO_2 solution	300 W Xe lamp (100 mW cm^{-2}, $\lambda \geq 420$ nm)	124.22	This work
$MAPbI_3$/RGO	HI/H_3PO_2 solution	300 W Xe lamp (120 mW cm^{-2}, $\lambda \geq 420$ nm)	939.00	[1]
$MAPbI_3$/Pt	HI/H_3PO_2 solution	Solar simulator (100 mW cm^{-2}, $\lambda \geq 475$ nm)	57.00	[2]
$CsPbBr_{3-x}I_x$/Pt	HBr/HI/H_3PO_2	300 W Xe lamp (	1120.00	[3]

	solution	$\lambda \geq 420$ nm)		
Pt/Ta_2O_5-$MAPbBr_3$-PEDOT:PSS	HBr/H_3PO_2 solution	300 W Xe lamp (150 mW cm^{-2}, $\lambda \geq 420$ nm)	619.00	4
$MAPbBr_{3-x}I_x/Pt$	$HBr/HI/H_3PO_2$ solution	300 W Xe lamp ($\lambda \geq 420$ nm)	2604.80	5
$MAPbI_3/Pt/TiO_2$	HI/H_3PO_2 solution	300 W Xe lamp (200 mW cm^{-2}, $\lambda \geq 420$ nm)	1987.00	6
$MAPb(I_{0.9}Br_{0.1})_3$	$HBr/HI/H_3PO_2$ solution	300 W Xe lamp ($\lambda \geq 420$ nm)	1471.00	7
$MAPb(I_{0.9}Br_{0.1})_3/Pt$	$HBr/HI/H_3PO_2$ solution	300 W Xe lamp ($\lambda \geq 420$ nm)	3348.00	7
$MAPbI_3/CoP$	HI/H_3PO_2 solution	150 W Xe lamp ($\lambda \geq 420$ nm)	2087.50	8
$MAPbI_3/Ni_3C$	HI/H_3PO_2 solution	300 W Xe lamp (100 mW cm^{-2}, $\lambda \geq 420$ nm)	2362.00	9
$MAPbI_3/MoS_2$	HI/H_3PO_2 solution	90 W LED lamp (450 mW cm^{-2}, 780 nm $\geq \lambda \geq$ 380 nm)	2061.00	10
$BP/MAPbI_3$	HI/H_3PO_2 solution	300 W Xe lamp (100 mW cm^{-2}, $\lambda \geq 420$ nm)	3742.0	11

References

1. Y. Wu, P. Wang, X. Zhu, Q. Zhang, Z. Wang, Y. Liu, G. Zou, Y. Dai, M.-H. Whangbo and B. Huang, *Adv. Mater.*, 2018, **30**, 1704342.
2. S. Park, W. J. Chang, C. W. Lee, S. Park, H.-Y. Ahn and K. T. Nam, *Nano Energy*, 2016, **2**, 16185.
3. Z. Guan, Y. Wu, P. Wang, Q. Zhang, Z. Wang, Z. Zheng, Y. Liu, Y. Dai, M.-H. Whangbo and B. Huang, *Appl. Catal., B*, 2019, **245**, 522-527.
4. H. Wang, X. Wang, R. Chen, H. Zhang, X. Wang, J. Wang, J. Zhang, L. Mu, K. Wu, F. Fan, X. Zong and C. Li, *ACS Energy Lett.*, 2019, **4**, 40-47.
5. Y. Wu, P. Wang, Z. Guan, J. Liu, Z. Wang, Z. Zheng, S. Jin, Y. Dai, M.-H. Whangbo and B. Huang, *ACS Catal.*, 2018, **8**, 10349-10357.
6. X. Wang, H. Wang, H. Zhang, W. Yu, X. Wang, Y. Zhao, X. Zong and C. Li, *ACS Energy Lett.*, 2018, **3**, 1159-1164.
7. Z. Zhao, J. Wu, Y.-Z. Zheng, N. Li, X. Li, Z. Ye, S. Lu, X. Tao and C. Chen, *Appl. Catal., B*, 2019, **253**, 41-48.
8. C. Cai, Y. Teng, J.-H. Wu, J.-Y. Li, H.-Y. Chen, J.-H. Chen and D.-B. Kuang, *Adv. Funct. Mater.*, 2020, **30**, 2001478.
9. Z. Zhao, J. Wu, Y.-Z. Zheng, N. Li, X. Li and X. Tao, *ACS Catal.*, 2019, **9**, 8144-8152.
10. F. Wang, X. Liu, Z. Zhang and S. Min, *Chem. Commun.*, 2020, **56**, 3281-3284.
11. R. Li, X. Li, J. Wu, X. Lv, Y.-Z. Zheng, Z. Zhao, X. Ding, X. Tao and J.-F. Chen, *Appl. Catal., B*, 2019, **259**, 118075.